Pergamon

Journal of Structural Geology, Vol. 18, Nos 2/3, pp. 343 to 348, 1996

0191-8141/96 $15.00 + 0.00

0191-8141(95)00116-6

A cellular automaton fracture model: the influence of heterogeneity in the failure process

S. A. WILSON*

Fault Analysis Group, Department of Earth Sciences, University of Liverpool, Liverpool L69 3BX, U.K.

J. R. HENDERSON

Department of Geological Sciences, The University of Durham, Durham DH1 3LE, U.K.

and

I. G. MAIN

Department of Geology and Geophysics, University of Edinburgh, Edinburgh EH9 3JW, U.K.

(*Received* 11 *February* 1995; *accepted in revised form* 23 *August* 1995)

Abstract—The modelling of a complex process such as rock fracture is fraught with problems including: (i) the number and complexity of the processes in operation during fracture; and (ii) the heterogeneity of the material under consideration. These considerations force modellers to adopt a 'notional' approach. In this paper we describe a model of fracture which attempts to mimic the processes that govern seismogenesis by using a rule-based algorithm. This allows us to capture the essential physical aspects of the system while allowing a realistic heterogeneity in the form of a large number of lattice elements. We describe the model and present the preliminary results from such a rule-based algorithm, or cellular automaton. These results illustrate that initial strength distributions have a crucial influence on the fracture pattern that is produced.

INTRODUCTION TO THE MODEL

This work derives from a purely two-dimensional lattice fracture model (Henderson *et al.* 1994) in which failure could take place only in mode I producing a plan view of the failure process. The inclusion of the BGK model for fluid flow (Bhatnager *et al.* 1954) allows the determination of fluid pressure at each lattice site and prompted the use of the Griffith-crack/Mohr–Coulomb failure criterion since effective stress could be calculated across the lattice. The use of this failure criterion also imparts a three-dimensionality to the model since failure can take place out of the σ_1–σ_2 plane. In order to accommodate the three-dimensionality introduced by using a Griffith-crack/Mohr–Coulomb failure criterion, the model may be thought of as representing small fractures in a developing fault zone and envisaged as the projection of this onto a two-dimensional visualization plane (Fig. 1). Thus adjacent elements on the lattice may fail in different orientations but as a whole it is assumed that they will eventually form part of one shear surface.

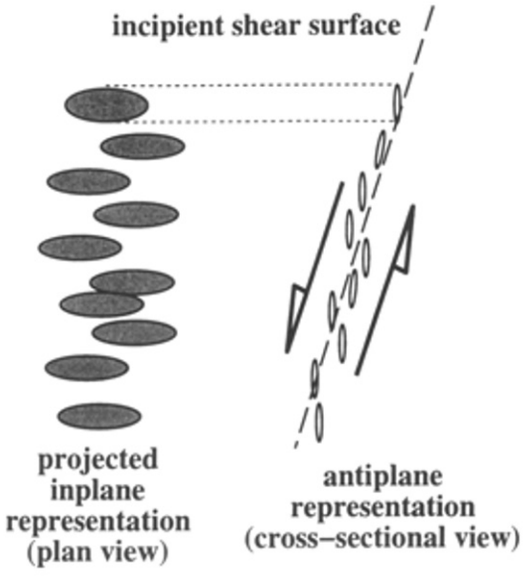

Fig. 1. A two-dimensional, anti-plane (i.e. cross-sectional) view of failure projected onto a two-dimensional visualization plane (plan view).

Failure of the model takes place by applying a slowly-increasing stress to the lattice. Each lattice element is assigned a notional tensile strength (cf. Initial Conditions) and fails whenever this strength is exceeded by

*Present address: CSMA Ltd, Rosemanowes, Hermiss, Penryn, Cornwall TR10 9DU, U.K.

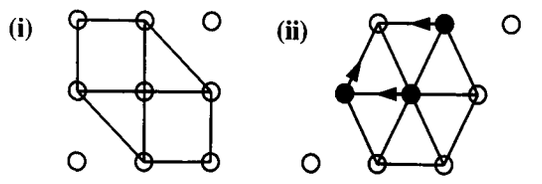

Fig. 2. (i) A 3 × 3 array of lattice elements containing one central element and defining its six nearest neighbours. (ii) The conceptual manner in which this lattice group is treated within the model illustrating the movement of fluid particles from lattice site to lattice site.

the applied stress. The load supported by this element is then transferred to its nearest neighbours. In this way stress becomes concentrated onto the stronger elements of the lattice causing an increased likelihood of unstable fracture propagation. In contrast to this process of increased instability, fluid pressure fluctuations temporarily halt this unstable propagation: whenever an element fails, fluid pressure at that site is reduced causing an influx of fluid from the surroundings, reducing fluid pressure and temporarily stabilising fracture propagation. These two processes, one causing temporary stability and one causing increased instability, control the behaviour of the model.

INITIAL CONDITIONS

In this preliminary study a number of strength distributions, some fractal and some non-fractal, are used to investigate the effect of the strength distribution on the resultant fracture population. These distributions consist of: (i) a spatially fractal distribution derived from a Gaussian model (Huang & Turcotte 1989); (ii) a Weibull distribution (Turcotte 1992) which is spatially non-fractal yet it has a fractal size distribution except at large values; (iii) a random uniform, and (iv) a random Gaussian distribution.

THE FLUID MODEL

As mentioned above, the model is based on a two-dimensional hexagonal lattice. This hexagonal format is achieved by ignoring the north-eastern and south-western elements of a 3 × 3 lattice group (Fig. 2). Computationally this arrangement is trivial yet it is fundamental to the functionality of the fluid model. The fluid model works by reducing fluid movements to particles of fluid which move around the lattice colliding with each other as the simulation progresses. Fluid pressure is derived from the probability of finding fluid particles at any site at any time. This model is derived from the FHP lattice model (Frisch *et al.* 1986) and the lattice Boltzmann model (Benzi *et al.* 1992).

THE FAILURE CRITERION

The failure criterion is based on a Griffith-crack/Mohr–Coulomb model giving a parabolic failure envelope from $T_0 \leq \sigma_n \leq -2T_0$, and a linear failure envelope from $\sigma_n \geqslant T_0$. This parabolic failure envelope is described by equation (1) and relates the shear stress, τ, to the normal stress, σ_n, given a tensile strength, T_0:

$$\tau^2 = 4T_0^2 - 4T_0\sigma_n. \quad (1)$$

For failure to occur the Mohr circle describing the load on an element must touch the failure envelope. Thus for tensile failure the minimum principal effective stress, $\sigma_3' = T_0$. For mixed mode failure $-T_0 < \sigma_{mean} < -2T_0$, where σ_{mean} is the mean stress. These simple comparative criteria make the determination of different failure types computationally very efficient. In this model it is assumed that $\sigma_1 \approx \sigma_2$.

Although the Griffith-crack/Mohr–Coulomb failure criterion is ideal for the purpose of modelling, it must be remembered that it does not provide an accurate model for microscopic failure and should not be used as such (Scholz 1990). Nevertheless it has a firm experimental basis and is appropriate for the scale of interest of this study.

RESULTS

Figure 3 shows the evolving fracture populations in plan view. Each of the four simulations is derived from each of the four different initial strength distributions. In order to remove the apparent anisotropy in these images and to display them in their true state they would need to be transformed in the same manner as that shown in Fig. 2. The spatial distributions of these fracture populations were analysed using the box counting method (Feder 1988). The size distribution of these populations were analysed in a similar way to that of earthquakes: by relating fracture area to seismic magnitude using the relationship, magnitude $\propto$ log (area) (Kanamori & Anderson 1975). If a straight line relationship is observed between log(N) and log(area) then the size distribution is fractal with the seismic b-value represented by the slope of this line. [N is the number of fractures greater than a particular area.]

In this study, fracture area is an integer variable, thus at small values the size distribution curve appears stepped. At large areas the number of such large fractures becomes under-represented since the size of the lattice is finite. This forces the size distribution curve to taper off at high area values. The decrease in the total number of fractures as each simulation progresses (Fig. 4) results from the coalescence of fractures.

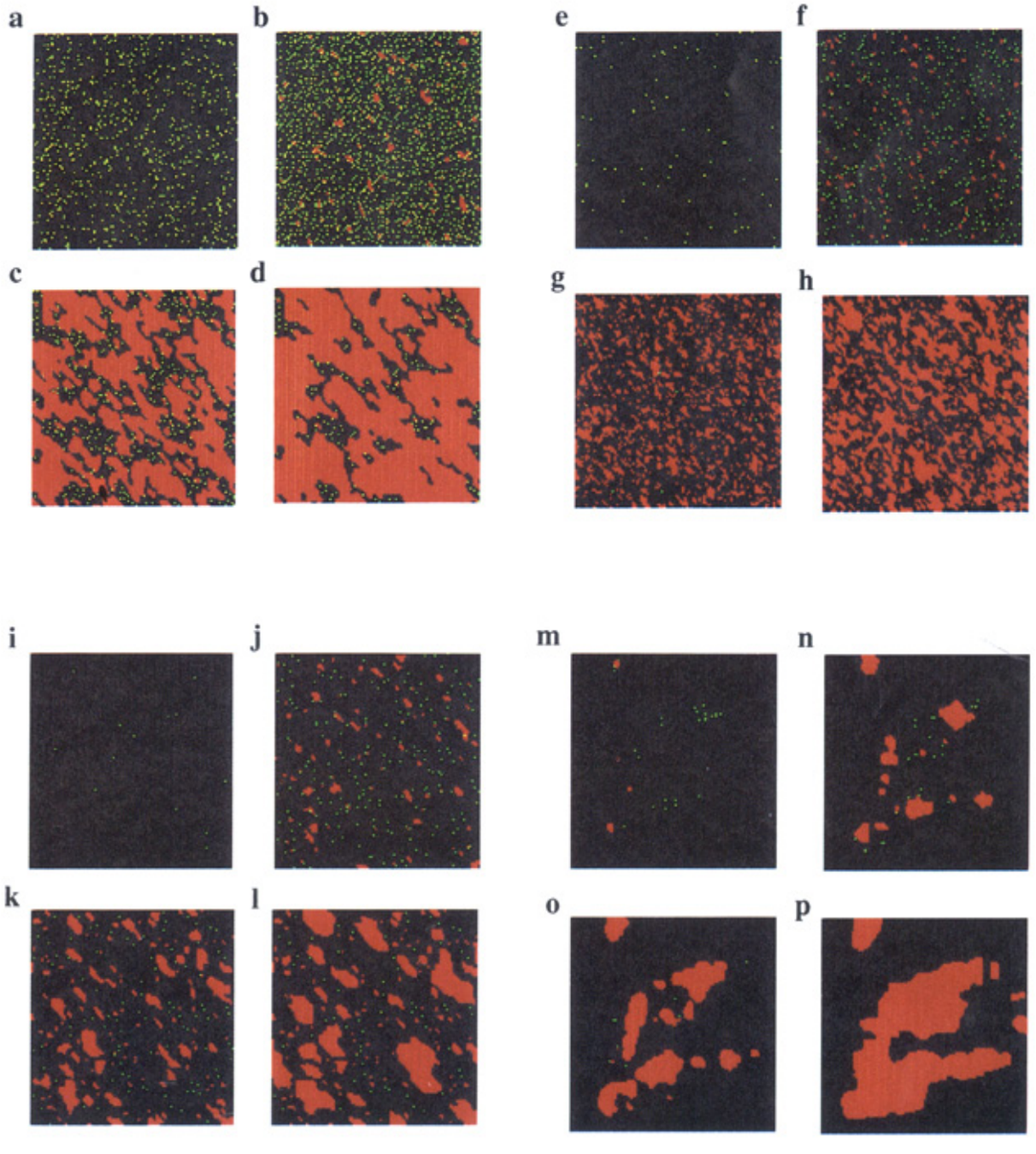

Fig. 3. The evolution of fracture populations using: (i) a Weibull strength distribution (a–d); (ii) a random uniform strength distribution (e–h); (iii) a random Gaussian strength distribution (i–l); and (iv) a spatially fractal strength distribution (m–p). Legend: red; lattice elements failing in shear; yellow, lattice elements failing in tension; and green; lattice elements failing in mixed mode.

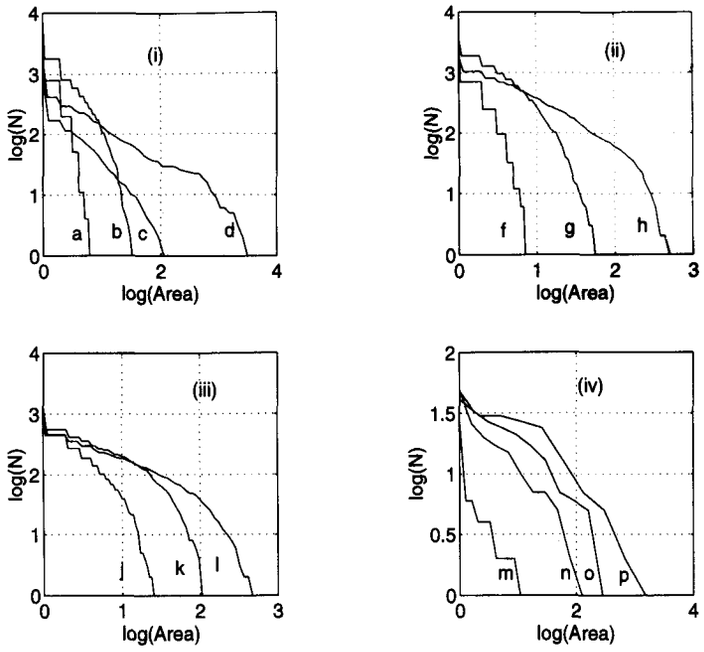

Fig. 4. Size distribution analyses of the fracture patterns shown in Fig. 3, where N is the number of fractures greater than area, and area is measured in the number of lattice elements.

SIZE DISTRIBUTION ANALYSES

The Weibull strength distribution

Initial failure is widespread and occurs in mixed mode (Fig. 3a). As the simulation progresses the applied stress and the differential stress increase making shear failure more likely. In Fig. 3(b) areas of mixed mode failure have begun to coalesce and now fail in shear. In Figs. 3(c) & (d) unstable shear crack propagation is taking place, i.e. failure continues without any increase in the applied stress.

The fracture size distribution during this simulation evolves toward a fractal population. During the initial phase described by curves a and b in Fig. 4, a best-fit curve to the data would have a continuously changing gradient and clearly describes a non-linear relationship. A best-fit curve to the data in Fig. 4(c) would have a fairly stable gradient from small areas until the curve tapers off as log(N) drops below 1. Curve d in Fig. 4 describes a linear relationship spanning two orders of magnitude where $0 < \log(\text{area}) < 2$ indicating a power-law size distribution between these limits.

The uniform random distribution

The size distributions (Figs. 4e–h) of the fracture patterns in Figs. 3(e)–(h) show similar characteristics to the previous example with an initial non-linear relationship (Figs. 4f–h) gradually changing to a more linear one. The last image shows a pronounced decrease in log(N) at log(area) > 2 (Fig. 4h) which is probably a result of the finite nature of lattice size.

The random Gaussian strength distribution

This strength distribution produces a very sparse fracture pattern which takes longer to reach instability. Once again the size distributions show an evolution from a non-linear to a linear relationship between log(N) and log(area) (Figs. 4j–l). However at the end of this simulation the straight line part spans only 1.5 orders of magnitude and rather than a rapid falloff at greater magnitudes the relationship has more of a gentle taper (Fig. 4l).

The fractal strength distribution

When failure first occurs it takes place in very localized regions corresponding to local minima in the strength distribution (Fig. 3m). These failed regions gradually enlarge and coalesce with failure changing from a mixed mode to a shear type mechanism (Fig. 3n). By the end of the simulation failure is concentrated in specific regions surrounded by the stronger parts of the lattice (Figs. 3o & p).

Although there is considerable fluctuation about any best-fit line, a generally linear relationship can be made out between log(N) and log(area) on the size distribution plots shown in Figs. 4(m)–(p). This consistently linear relationship throughout the simulation contrasts with the behaviour of the other simulations described earlier whereby size distributions evolve toward a power-law relationship over time.

The evolving pattern may be used as a first approximation to justify the fault growth model of Gillespie *et al.* (1992), where the b-value remains relatively constant as the maximum fault length grows.

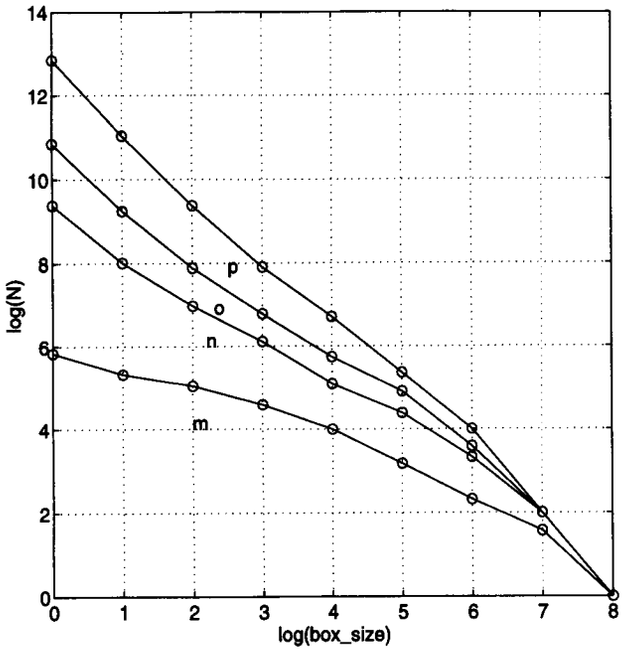

Fig. 5. Box counting analysis of the fracture patterns shown in Figs. 3(m–p), where N is the number of filled boxes and box size is measured in lattice elements.

ANALYSIS OF SPATIAL DISTRIBUTIONS

All the strength distributions with uncorrelated spatial distributions produced non-fractal spatial fracture populations. Box counting analysis of the failure distributions for the fractally-distributed strength distribution produced generally linear functions within the central portion of the box size range (i.e. $6 > \log(\text{box size}) > 2$). The gradients of these functions demonstrate a change in fractal dimension from 0.6 to 1.6 as the simulation progresses (Fig. 5).

CONCLUSION

Size distribution analysis demonstrates that spatially uncorrelated strength distributions produce fracture populations that evolve toward a power-law size distribution, whereas the spatially correlated distribution produces consistent power-law size distributions throughout its evolution. Box counting analysis demonstrates that the spatial fracture distribution is dependent on the initial heterogeneity: the spatially correlated strength distribution produces a spatially correlated fracture population: the spatially uncorrelated strength distributions result in spatially uncorrelated fracture populations. The disposition of initial heterogeneities, which is something that we know little about in nature, has a crucial effect on fracture populations.

Acknowledgements—The authors would like to thank Kes Heffer at BP Research and Elf Aquitaine for the provision of funds for this research.

REFERENCES

Benzi, R., Succi, S. & Vergassola, M. 1992. The lattice Boltzmann equation: theory and applications. *Phys. Rep.* **22**, 145–197.

Bhatnager, P. L., Gross, E. F. & Krook, M. 1954. A model for collision processes in gases. *Phys. Rev.* **94**, 511–525.

Feder, J. 1988. *Fractals*. Plenum Press, New York.

Frisch, U., Hasslacher, B. & Pomeau, Y. 1986. Lattice-gas automata for the Navier–Stokes equation. *Phys. Rev. Lett.* **56**, 1505–1509.

Gillespie, P. A., Walsh, J. J. & Watterson, J. 1992. Limitations of dimension and displacement data from single faults and the consequences for data analysis and interpretation. *J. Struct. Geol.* **14**, 1157–1172.

Henderson, J. R., MacLean, C., Main, I. G. & Norman, M. G. 1994. A fracture-mechanical cellular Henderson, J. R., MacLean, C., Main, I. G. & automaton model of seismicity. *Pure & Appl. Geophys.* **142**, 545–565.

Huang, J. & Turcotte, D. L. 1988. Fractal distributions of stress and strength and variations of *b*. *Earth Planet Sci. Lett.* **91**, 223–230.

Kanamori, H. & Anderson, D. L. 1975. Theoretical basis of some empirical relations in seismology. *Bull. seism. Soc. Am.* **65**, 1073–1096.

Theoretical basis of some empirical relations in seismology. *Bull. seism. Soc. Am.* **65**, 1073–1096.

Scholz, C. H. 1990. *The Mechanics of Earthquakes and Faulting*. Cambridge University Press, Cambridge.

Turcotte, D. L. 1992. *Fractals and Chaos in Geology and Geophysics*. Cambridge University Press, Cambridge.